Immobilisation of single molecule magnets in mesoporous silica hosts

Stephanie Willemin,[a] Guillem Arrachart,[a] Lollita Lecren,[b] Joulia Larionova,*[a] Thibaud Coradin,*[c] Rodolphe Clérac,[b] Talal Mallah,[d] Christian Guérin[a] and Clément Sanchez[c]

[a] *Laboratoire de Chimie Moléculaire et Organisation du Solide, CNRS-UMR 5637, Université de Montpellier II, place E. Bataillon, F-34095, Montpellier cedex 5, France. E-mail: joulia@univ-montp2.fr; Fax: +33 4 671438 52; Tel: +33 4 67144824*

[b] *Centre de Recherche Paul Pascal, CNRS-UPR 8641, 115 Avenue du Dr Schweitzer, F-33600, Pessac*

[c] *Laboratoire de Chimie de la Matière Condensée, CNRS-UMR 7574, UPMC, 4 place Jussieu, F-75252, Paris, France. E-mail: coradin@ccr.jussieu.fr; Fax: +33 1 44274769; Tel: +33 1 44275517*

[d] *Laboratoire de Chimie Inorganique, CNRS-UMR 8613, Université Paris-Sud, F-91405, Orsay, France*

Received (in Montpellier, France) 7th May 2003, Accepted 2nd July 2003
First published as an Advance Article on the web 1st September 2003

Molecular clusters $[Mn_{12}O_{12}(RCOO)_{16}(H_2O)_n]$ (R = CH_3, C_6H_5 ($n = 4$) and C_2H_5 ($n = 3$)) and $[Mn_4(CH_3COO)_2(pdmH)_6]$ (pdmH = 2,6-bis (hydroxymethyl)pyridine) presenting Single Molecule Magnetic (SMM) behaviour were inserted into hexagonal mesoporous silica with pore size in the 25–100 Å range. An optimum host pore size exists which maximizes the amount of embedded cluster. The composites were studied by X-ray diffraction, infrared spectroscopy, magnetic measurements, nitrogen sorption, thermogravimetric analysis and transmission electronic microscopy. All these methods reveal the presence of intact guest clusters inside the silica pores. Moreover, if the magnetic properties of the clusters appear globally unmodified by the insertion process, the absence of a magnetic isomer form of $[Mn_{12}O_{12}(CH_3COO)_{16}(H_2O)_4]$ within silica porosity suggests an influence of the confinement on the cluster structure.

Introduction

The design of novel host–guest compounds with unusual physical or chemical properties is of considerable interest in contemporary science.[1] In such compounds, organization at the molecular level is achieved by host–guest interactions which span the full range from weak van der Waals coupling to strong electrostatic interactions. Ordered porous host matrices are well suited for the rational design of new composites, as they can be easily processed in a wide range of structures (pore size and organization) and shapes (bulk, films, fibres).[2] Design considerations can then focus on the optimisation of geometrical fit between the pore system and the guest, and the tuning of host–guest interactions.

Among the host systems, ordered mesoporous silicas have attracted much interest, since they possess well-defined voids accessible for the guest components, good chemical, thermal and mechanical stability.[3] If numerous organic and bio-organic molecules have been successively introduced into silica hosts,[4,5] reports on the immobilisation of inorganic species (coordination compounds, organometallics, polyoxometalates, clusters) are much more limited.[6]

In this context, we have previously reported the successful incorporation of nanoclusters presenting unusual magnetic properties defined as "Single Molecule Magnet" (SMM) into hexagonal mesoporous silica hosts.[7] The synthesis and studies of SMM has become an area of intense research, since the discovery that such molecules can act as nanoscale magnets below a critical temperature ("blocking temperature").[8] These molecules have a large ground spin state and strong uni-axial anisotropy resulting in a barrier for spin reversal.[9] This feature is characterized by a slow relaxation of the magnetization which gives rise to a "metastable magnet" with hysteresis effects similar to those observed in bulk magnets. Additionally, these molecules display quantum tunnelling of magnetization and quantum phase interference.[10,11] This behaviour is due to individual molecules rather than to long-range ordering, as confirmed by magnetization relaxation and heat-capacity studies.[12] Therefore, SMMs represent nanoscale magnetic objects of a sharply defined size that offer new possibilities to high-density information storage at the molecular level[13] and quantum-computing applications.[14] However, these applications require the control and organization of oriented molecules or molecular aggregates in material where each individual species can be used as a bit of information. An interesting approach to arrange molecules into organized multilayered films has been performed using Langmuir–Blodgett films[15] and polymeric thin films.[16] Alternatively, using mesoporous hosts should allow the organisation of SMM at the nanometer scale, considering the host framework as a template for the arrangement of guest species.

Organization and orientation effects will probably only be achieved using anisotropic mesoporous materials, such as thin films. However, it is first necessary to get a better insight of the cluster-silica interactions. We have previously shown that the incorporation of nanoclusters into mesoporous hexagonal silica powders maintains the integrity of the host phase as well as that of the incorporated clusters.[7] Such preliminary results encourage us to further investigate these magnetic composite systems and extend this approach to other magnetic molecular guests.

In this work, the incorporation of two families of high spin manganese carboxylate cluster presenting SMM behaviour, $[Mn_{12}O_{12}(RCOO)_{16}(H_2O)_n]$ with R = CH_3,[17] C_6H_5 (n = 4),[18] C_2H_5 (n = 3)[19] and $[Mn_4(CH_3COO)_2(pdmH)_6]$ (pdmH = 2,6-bis (hydroxymethyl) pyridine),[20] in silica mesoporous hosts of various pore sizes was studied. In a first step, we have tried to adapt the host structural features with cluster size and nature in order to optimize cluster incorporation. In a second step, X-ray powder diffraction, porosity measurements and Transmission Electron Microscopy allowed confirmation of the presence of clusters within the silica host whose structure has been maintained during the insertion process. Finally, infrared spectroscopy, thermogravimetric analysis and magnetic susceptibility measurements indicate that the cluster molecular structure is not modified within the mesoporous network. Nevertheless, the absence of a magnetic isomer of $[Mn_{12}O_{12}(CH_3COO)_{16}(H_2O)_4]$ after insertion suggests that the host lattice may, at least partially, control cluster structure.

Experimental

Cluster synthesis

$[Mn_{12}O_{12}(CH_3COO)_{16}(H_2O)_4]\cdot 2CH_3COOH\cdot 4H_2O$[17] (**1**), $[Mn_{12}O_{12}(EtCOO)_{16}(H_2O)_3]\cdot 4H_2O$[19] (**2**), $[Mn_{12}O_{12}(C_6H_5COO)_{16}(H_2O)_4]\cdot 2CH_3COOH\cdot 4H_2O$[18] (**3**) and $[Mn_4(CH_3COO)_2(pdmH)_6]$ (pdmH = 2,6-bis(hydroxymethyl)pyridine)[20] (**4**) were prepared following literature procedures.

Mesoporous hosts synthesis

SBA-15 type mesoporous silica with pore size D_p ranging from 25 Å to 100 Å, hereafter denoted SBA(D_p), were prepared following the procedure of Zhao *et al.* using a non ionic alkyl poly(ethylene oxide) surfactant (Brij 56, Aldrich) and a triblock copolymer (P 123, Aldrich).[21] Removal of organic templates was performed by calcination at 500 °C.

Cluster insertion

The incorporation of the **1**, **2**, **3** and **4** into mesoporous silica was performed by adding the silica powder to a saturated solution of the complex in dry solvent. The mixture was stirred for 2 h at room temperature in a closed flask. After filtration, the brown powder was thoroughly washed several times with solvent until the filtrate became colorless and dried at room temperature for 2 h in vacuum. CH_3CN was used as solvent for **1** and **4**, and CH_2Cl_2 for **2** and **3**. Resuspension of the nanocomposites for 24 hours in the corresponding insertion solvent was carried out to check the strength of the cluster–silica interaction.

Physical measurements

Infrared spectra were recorded as KBr disks or Nujol mulls between KBr plates on a Perkin Elmer 1600 spectrophotometer. Thermogravimetric (TG) analysis was performed using Netzsch STA 409 Thermobalance instrument under argon in the 30–500 °C range with a 1 °C min^{-1} heating rate. Powder X-ray diffraction (XRD) data were recorded on a Philipps Xpert diffractometer, using a Cu target and a back monochromator ($K\alpha_1 + K\alpha_2$) in the 0.5–88° 2θ range (Institut Européen des Membranes, Montpellier, France). Nitrogen sorption experiments were performed at 77 K on a Micromeretics ASAP 2010 and Micromeritics Gemini III 2375 analysers. Specific surface areas (S_{BET}) were determined by the BET method,[22] porous volume (V_p) and pore size (D_p) were calculated by the BJH model on the adsorption branch.[23]

Magnetic susceptibility data was collected with a Quantum Design MPMS-XL SQUID magnetometer in a temperature range of 1.8–350 K and up to 5 T. AC measurements were performed in 0.3 mT ac field with an ac frequency ranging from 1 to 1500 Hz without dc field. Experimental data were corrected for sample holder and for diamagnetic contribution calculated from Pascal constants.[24]

Transmission Electron Microscopy (TEM) has been performed on a High Resolution Transmission Electron Microscope CM 20 working at 200 kV and on a Transmission Electron Microscope JEOL 1200 EXII) working at 100 kV. Samples for TEM measurements were performed using ultramicrotomy techniques and then deposited on copper grids.

Elemental analysis were performed by the Service Central d'Analyse (CNRS, Vernaison, France).

Results

Optimization of cluster incorporation

The insertion of cluster **1** into mesoporous silica hosts with a large range of pore sizes varying from 25 to 100 Å was first performed by adding the mesoporous silica powder to a saturated acetonitrile solution of **1** for 2 h at room temperature. These conditions were fixed taking into account the solubility and the stability of **1**.

The Mn : Si atomic ratio in the nanocomposites was obtained from elemental and EDAX analysis, from which cluster amount in weight percent (wt %) could be calculated (Table 1). The amount of immobilised clusters appears to highly depend on host porosity. No insertion could be observed using SBA(25), cluster adsorption on the silica surface probably accounting for the low (0.5 wt %) measured amount of cluster. For larger pore sizes, the amount of inserted clusters first increases, reaching a maximum value for D_p = 60 Å, and then decreases, as shown on Fig. 1. A maximum Mn : Si atomic ratio of 18 : 20 is obtained, corresponding to 0.018 mol of **1** per mol of SBA(60), or 36 wt % of inserted cluster.

Keeping SBA(60) as the host phase, the reaction conditions (temperature, reaction time, initial concentration, solvent) have been varied in order to increase the inserted quantity of cluster. The insertions performed under mild heating (323 K) lead to the decomposition of **1**, but this was also observed in the absence of the silica powder. As far as insertion time is concerned, the maximum incorporation is achieved after 2 hours. Longer reaction times do not improve the amount of inserted clusters and even induce decomposition after 24 h.

The influence of the initial cluster concentration (Fig. 2) shows that the maximal insertion is reached for a concentration of 15 g L^{-1}. The EDAX analysis shows that the

Table 1 Amount of inserted clusters, in wt %, for different composites, before and after resuspension

		Inserted cluster (wt %)	
Cluster	D_p/Å	before resuspension	after resuspension
1	25	0.5	0.5
1	40	20.5	14.0
1	50	29.5	18.5
1	60	34.0	21.5
1	70	32.0	19.5
1	100	15.0	12.0
3	40	16.0	10.0
3	50	17.5	10.5
3	100	16.5	10.5
4	25	7.5	3.5
4	40	19.0	17.5
4	50	26.5	21.0
4	60	28.5	22.5
4	70	27.0	19.0

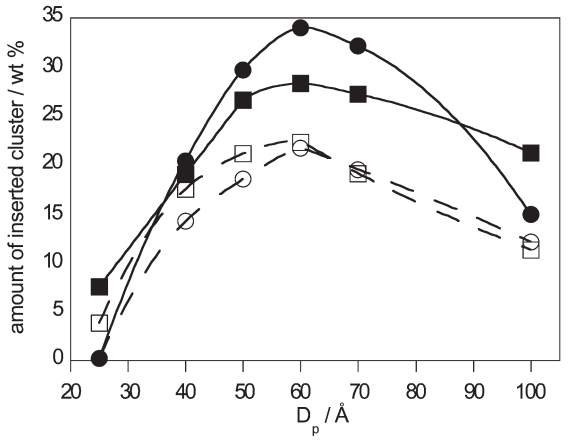

Fig. 1 Evolution of the amount of inserted cluster **1** and **4** (in wt %) with mesoporous silica pore size D_p, (●) cluster **1** before and (○) after resuspension; (■) cluster **4** before and (□) after resuspension.

composites obtained using initial concentration below this threshold value are all homogeneous. Increasing the concentration above 15 g L^{-1} induces the crystallisation of **1** on the surface of the silica host, as shown by EDAX analysis. It is worth noting that repeating the insertion process of **1** in the same conditions does not permit to increase the amount of inserted clusters.

The insertion of **2**, **3** and **4** in SBA(D_p) has been performed in order to vary cluster size and stability as well as reaction solvent. All tests for the insertion of **2** using CH_2Cl_2 and CH_3CN as solvents produce its decomposition, whereas it is stable over days in the absence of silica. The insertion of **3** using CH_2Cl_2 gives the composite materials but the quantity of inserted cluster is low (17 wt %). Cluster **4** has been confined in SBA hosts under the same conditions as for **1**. A similar pore size dependence of the inserted amount of clusters is observed (Fig. 1), up to 28 wt % being inserted in SBA(60) (Fig. 1, Table 1). Moreover, it is worth noticing that, in contrast to **1**, a noticeable amount of **4** (7.5 wt %) could be inserted in SBA(25).†

The 24 hours resuspension process led to an important decrease in cluster content for all the hosts but this leaching was more important for large quantity of inserted cluster indicating weak host–guest interactions within the nanocomposites. The remaining quantity of clusters **1** and **4** after intensive washing is reported in Fig. 1 and Table 1. Moreover, the washing solutions were found to mainly contain decomposed clusters.

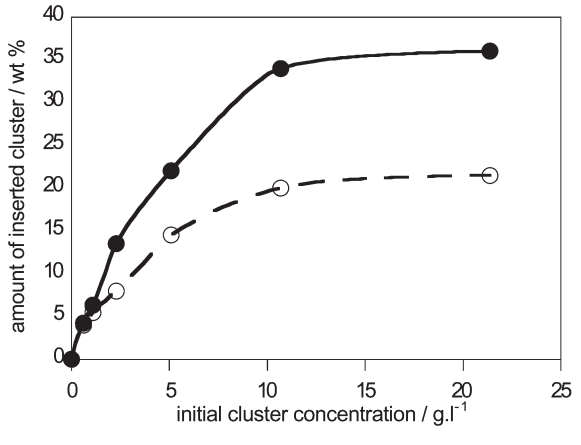

Fig. 2 Evolution of the amount of inserted cluster **1** (in wt %) with initial cluster concentration in SBA(60), (●) before and (○) after resuspension.

† It is to be noted that, because of the low amount of inserted cluster, χ'' measurements for **4** in SBA(25) did not allow a firm conclusion about the full integrity of the cluster in this porous network.

Structural characterisation of the nanocomposites

Fig. 3 shows the XRD patterns obtained for SBA(60) and the composite **1**-SBA(60) with maximum cluster **1** loading (36 wt %). The diffractogram for the pure silica displays five peaks due to the 100, 110, 200, 210, and 300 reflections of the hexagonal structure. Upon insertion, no shift of peak positions is observed. Moreover, no peaks could be detected above $2\theta = 5°$, suggesting the absence of cluster crystallisation at the surface or within the pores of the silica host.

Specific surface area and porous volume for SBA(*Dp*) used in this work together with **1**-SBA(60) and **4**-SBA(60) are gathered on Table 2 and the corresponding isotherms for SBA(60) and **1**-SBA(60) are shown on Fig. 4. The isotherm of SBA(60) has an H2 shape characteristic of SBA-15.[21] Upon insertion, the hysteresis part of the isotherm becomes flatter, taking on an H4 shape associated with slit-shaped mesopores.[25] Such a change suggests that the insertion of **1** alters the shape of the accessible pores. In addition, incomplete closure of the isotherm during desorption is observed which may indicate partial closure of the pores by occluded particles. Accordingly, a decrease in surface areas and pore volumes is observed after cluster insertion. Similar results were obtained for silica hosts containing **4**.

The TEM image for **1**-SBA(60) is shown in Fig. 5a. No visible clusters separated out on the surface of pores can be observed. Moreover, dense nanoparticles in the 30–40 Å size range, which appear to fill the pores of the silica porous network are observed. Even though image resolution does not allow a firm conclusion, these nanoparticles might correspond to aggregates of clusters. The atomic ratio Mn : Si given by EDS measurements is 18 : 82. The TEM image of **4**-SBA(60) is shown in Fig. 5b. As in the case of **1**-SBA(60), no visible particles separated out on the surface of pores. Although the particles of **4** inside of the pores cannot be found, a distinctive signal of manganese is detected by the EDAX measurement, the atomic ratio Mn : Si being always 6 : 94. This provides further evidence that most of the clusters **4** are homogeneously confined into the pore channels.

Influence of insertion on cluster properties

The presence of intact molecular clusters into the silica network could first be ascertained by infrared spectroscopy. Fig. 6a shows the infrared spectrum of **1**. Low frequency bands in the 500–700 cm^{-1} range (564 cm^{-1}, 608 cm^{-1}, 640 cm^{-1}, 675

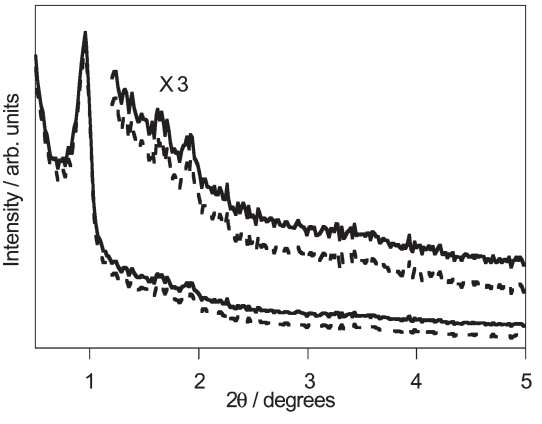

Fig. 3 X-Ray diffraction pattern for SBA(60) (—) and composite **1**-SBA(60) (---).

Table 2 Average pore diameter (D_p), specific surface area (S_{BET}) and porous volume (V_p) for the starting SBA(D_p) host and for SBA(60) incorporating cluster **1** and **4**

	D_p/Å	V_p/cm^3 g^{-1}	S_{BET}/m^2 g^{-1}
SBA(25)	25	0.40	600
SBA(40)	40	0.50	600
SBA(50)	50	0.70	670
SBA(60)	60	0.95	690
SBA(70)	70	1.05	790
SBA(100)	100	1.80	1390
1-SBA(60)	55	0.60	400
4-SBA(60)	55	0.75	460

cm^{-1}, 713 cm^{-1}) correspond to Mn–O stretches of the cluster core whereas the 1400–1550 cm^{-1} (1448 cm^{-1}, 1549 cm^{-1}, 1558 cm^{-1}, 1568 cm^{-1}) bands reflect the carbonyl group vibrations.[17–19] Identification of these bands for inserted clusters was also possible on the **1**-SBA(60) spectra together with SiO_2 vibration bands at 1080 cm^{-1}, 960 cm^{-1} and 800 cm^{-1} (Fig. 6b), but they appear more clearly when pure SBA(60) spectra was substracted (Fig. 6c). It is remarkable that wavenumber shifts for Mn–O core bands were always less than 2 cm^{-1}, suggesting that it is fully conserved within the mesoporous host.

The thermogravimetric analyses of **1** and **1**-SBA(60) performed under argon atmosphere from room temperature up to 500 °C are shown on Fig. 7. The pristine cluster exhibits three well-pronounced weight loss steps starting at 95 °C (11.5 wt %), 180 °C (14.4 wt %) and 260 °C (27.0 wt %). The first loss was attributed to the departure of acetic acid and water molecules present in crystal structure of the cluster, whereas the second correspond to partial elimination of acetic acid peripheral ligands.[26] At higher temperatures, decomposition of the cluster manganese-oxo core occurs leading to different Mn-oxides. In contrast, the TG curve for **1**-SBA(60) is much more complex, with somehow poorly defined steps. A first loss below 75 °C (9 wt %) can be attributed to CH_3CN molecules weakly adsorbed on the silica surface. Between 75 °C and 165 °C, a slow departure of matter, accounting for about 7 wt % of total weight, is observed. It is interesting to note that the loss step corresponding to outer CH_3COOH and H_2O molecules found for the pristine cluster powder do not appear clearly here. It seems reasonable to assume that, upon dissolution, these molecules leave the cluster proximity to be replaced by solvating CH_3CN molecules so that this weight loss may corresponds to acetonitrile molecules adsorbed on the surface and/or at the vicinity of inserted

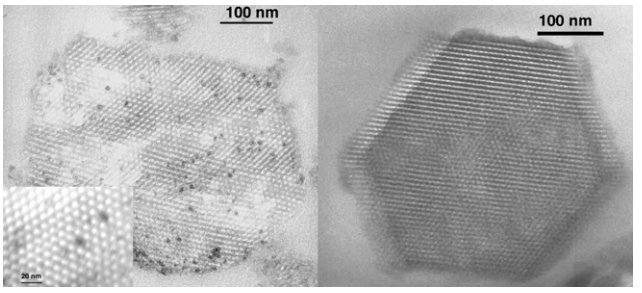

Fig. 5 (a, left) TEM image of **1**-SBA(60). Scale bar = 100 nm (inset: scale bar = 20 nm); (b, right) TEM image **4**-SBA(60). Scale bar = 100 nm.

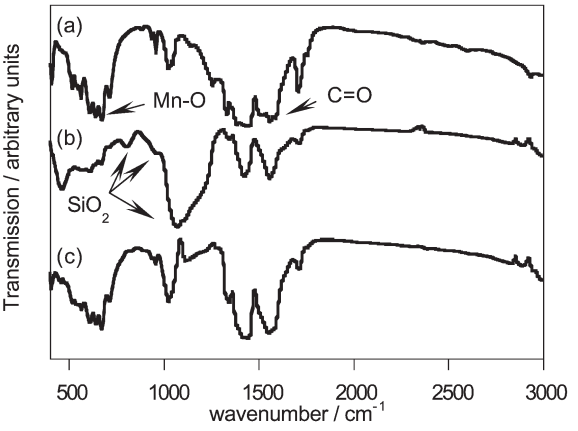

Fig. 6 Infrared spectra of (a) **1**, (b) **1**-SBA(60) and (c) difference spectra of **1**-SBA(60) with SBA(60).

clusters. In contrast, the subsequent step observed for **1**-SBA(60) at 165 °C with respective weight loss of about 6 wt % could correspond to the second of **1** at 180 °C (14.4 wt %), indicating that the cluster molecular structure is maintained within the host phase. However, the last step found at 260 °C for the pristine cluster appears now splitted in a two step process, therefore suggesting that the decomposition of this structure is modified by the interaction with the silica host.

The temperature dependence of the in-phase, χ', and out-of-phase, χ'', ac magnetic susceptibility for **1** inSBA(60) have been monitored in a zero external field with different frequencies ranging from 1 to 1500 Hz (Fig. 8). At 1 Hz, both, χ', the in-phase and χ'', the out-of-phase responses exhibit peaks at 5.11 and 4.52 K, respectively. These peaks shift towards higher

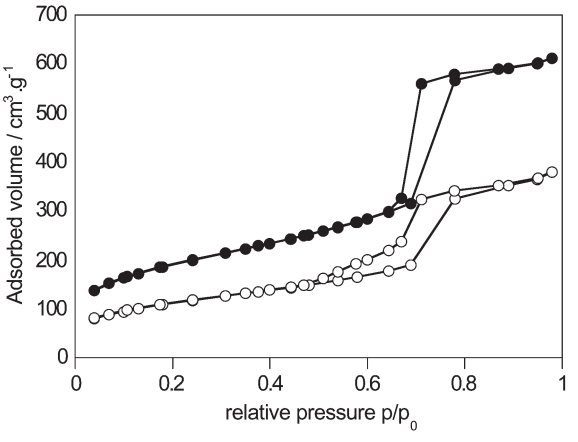

Fig. 4 Nitrogen sorption isotherm plots for SBA(60) (●) and composite **1**-SBA(60)(○).

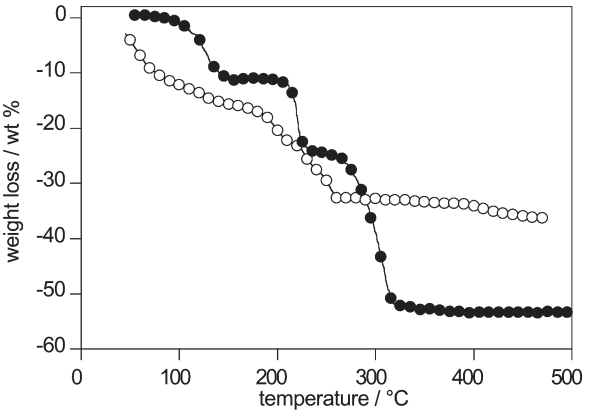

Fig. 7 Thermogravimetric analyses of **1** (●) and composite **1**-SBA(60)(○).

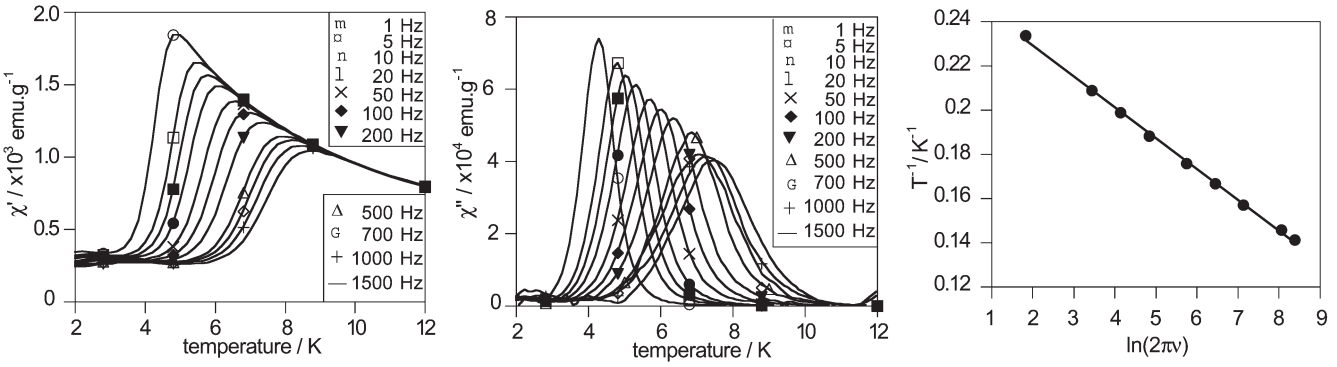

Fig. 8 Temperature and frequency dependence of (a) the real (χ') component and (b) the imaginary (χ'') component of the ac susceptibility for a sample of **1**-SBA(60) (Solid lines are guides), and (c) corresponding $ln(2\pi\nu)$ *vs.* $1/T_B$ plots of **1**-SBA(60). (Solid line represents the least-square fit of the experimental data to the Arrhénius equation (see text)).

temperature when the frequency increases, as also observed in **1**. This feature is characteristic of super-paramagnetic like behavior (or SMM behavior). From the frequency dependence of these peaks, we show that the relaxation time of **1** within the silica host follows an Arrhenius law, $\tau = \tau_0 \exp(\Delta/k_BT)$, with activation energy, $\Delta = 72$ K and pre-exponential factor, $\tau_0 \approx 1.03 \times 10^{-8}$ s (Fig. 8c). These parameters are close to these observed for **1** *i.e.* with $\Delta = 69$ K and $\tau_0 \approx 1.2 \times 10^{-8}$ s. The slight differences in these parameters, compared to the high sensitivity of a single molecule magnet behaviour, may be due to the absence in the composite of inter-cluster solvent molecules (water and acetic acid), in agreement with TG analysis. It is interesting to note that the low-temperature relaxation process always present in **1** ($\Delta = 37.1$ K and $\tau_0 \approx 8.0 \times 10^{-10}$ s) and attributed to the existence of an isomer form of the cluster of **1** in the solid-state is not observed after insertion inSBA(60).[26] Finally, the shape and the coercive field of the hysteresis loop for **1**-SBA(60) measured at 1.8 K, shown in Fig. 9, are similar to what was observed for **1**. The complex form of the hysteresis can be attributed to the fact that the cluster still exhibits rotational freedom within the pores so that it can be oriented by the applied magnetic field.‡

Discussion

The successful immobilization of inorganic clusters within mesoporous hosts depends on several factors that have clearly appeared in this work. From a geometrical point of view, optimization of the porosity can not only rely on the cluster size. The largest dimension of **1** is about 17 Å, not taking into account hydrogen atoms. However, it could not be inserted in SBA(25) and showed an optimum pore size $Dp = 60$ Å. As a comparison, **4**, which is smaller by only *ca.* 4 Å can be inserted in SBA(25), but exhibits the same optimum host pore size. This can be attributed to the fact that the clusters enter the porous network surrounded by their solvation shell, which increases their overall dimensions. In this context, it is interesting to note that it was possible to insert polyoxoanions of *ca.* 20 Å large in MCM-41 pores of *ca.* 21 Å using water as a solvent.[6f] Moreover, nitrogen sorption analysis provides an average pore size but it might be more relevant to consider the small-diameter side of the pore distribution, especially if it indicates the presence of narrower necks in the porous network. Thus, a minimum pore size is needed for insertion to occur but, above a given optimum value, larger cavities lead to a decrease of the amount of immobilized species, as illustrated for **1** and **4**. It can be suggested that larger pores ease the leaching of clusters during the insertion process. As a result, less molecules can be trapped but these molecules will be more difficult to remove. For example, it is possible to insert *ca.* 35 wt % of **1** in SBA(60), this amount being reduced to *ca.* 20 wt % after resuspension. In contrast, only *ca.* 15 wt % of the same cluster is immobilized in SBA(100) but *ca.* 12 wt % remain in the resuspended powder.

Another crucial point is the nature of the interaction between the host surface and the cluster. Decomposition of **2** in the presence of the silica powder suggests that the surface silanol groups may be detrimental to its stability. These interactions also determine the amount of immobilized clusters. Thus, it is possible to insert about twice as much cluster **1** than **3**, even though their sizes differ only by less than 5 Å and this may be attributed to unfavorable interactions between the silica surface and phenyl groups of **3** outer-shell. Accordingly, the presence of hydroxyl groups on the pdmH ligand of **4** should lead to hydrogen bond formation with host silanol groups. As a consequence, upon resuspension of **4**-SBA(60), the amount of inserted clusters is only reduced by *ca.* 20% compared to *ca.* 40% for **1** in the same host. In this context, the possibility to incorporate a carboxilic acid functionality on the silica surface should allow a better anchorage of the clusters.

As far as the host network is concerned, the whole pore structure appears maintained during the insertion process. Nitrogen adsorption nevertheless suggests that some of the pores are filled with clusters, as confirmed by TEM. The observed slit-shaped pores may arise from the fact that *ca.* 15 Å clusters will not occupy the whole 60 Å pore space so that

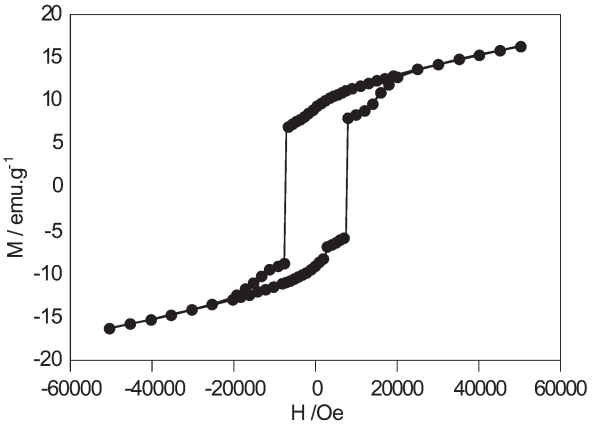

Fig. 9 Hysteresis loop for **1**-SBA(60)at 1.8 K.

‡ Ac susceptibility measurements were also undertaken on **4** in SBA(60). However, this cluster exhibits lower blocking temperatures (2.03 K at 995 Hz; 1.16 K at 1.1 Hz) than **1**, so that the low frequencies data could not be fully recorded, preventing the determination of Δ and τ_0. Nevertheless, measurements performed at high frequencies were consistent with reported data for pristine **4**.[20]

the remaining surface should be accessible for the gas analysis. On the contrary, as mentioned above, the smallest cavities of the pore size distribution should be fully capped by the inserted molecules, explaining the absence of closure of the adsorption–desorption curve.

Finally, investigations of the clusters structure and magnetic properties within the mesoporous network tend to demonstrate that they are unmodified by the insertion process. However, we have noticed the absence of one of the magnetic isomer of **1**. These isomers were reported for several Mn_{12} SMM in the solid-state and shown to depend on the arrangement of water and carboxylate ligands around the Mn–O core.[27] It was also indicated that the two isomers exist in solution. However, in the case of **1**, the two isomer forms could not be separated and were observed even after outer water and acetate departure.[26] Therefore, since, for this particular cluster, the nature of the two forms is still controversial, it can only be suggested that the confinement of the cluster and/or the chemical environment provided by the pores favor one of the isomers.

Conclusion

The concept of using the well-organized pore systems of mesoporous SiO_2 frameworks as templates for arrangement of guest molecules offer a new synthetic route to host–guest compounds with very weak host–guest interactions and reduced guest–guest interactions. By choosing the appropriate pore systems, the design of a specific assembly of host–guest systems becomes possible. Hypothetically, the confinement and the organization of SMM materials in host matrices could lead to: (i) the intrinsic response of SMM; (ii) the inter-cluster distance control; (iii) the increase of the anisotropy by a minimization of the distribution of the easy magnetization axis orientations of each cluster; (iv) the control of the relaxation processes; (v) the processability and the protection of the clusters. In this work, three manganese-based SMM, $[Mn_{12}O_{12}(RCOO)_{16}(H_2O)_4]$ ($R = CH_3$, C_6H_5), and $[Mn_4(CH_3COO)_2(pdmH)_6]$ were incorporated in mesoporous silica with pore sizes ranging from 25 Å to 100 Å. We show that an optimum host pore size exists which maximizes cluster insertion. Overall magnetic properties of the clusters are revealed to be unmodified by the insertion process but one of the two cluster magnetic isomers appears to be favored within the pores.

It is nevertheless worth noting that if this approach appears successful in elaborating materials where SMM are isolated, no control of the inter-cluster distance and/or the organization of these clusters inside of the pores have yet been achieved. We are currently studying the possibility to immobilise SMM systems in mesoporous thin films where lower dimensionality of the host should reduce the spatial distribution of the inserted species and may therefore provide an adequate medium for a better control of cluster organization and orientation.

Acknowledgements

T. C. thanks K. Benzerara for his help in TEM studies. J. L and S. W. thank Y. Guari for TEM measurements and discussions. R. C. and L. L. would like to thank the CNRS and the Conseil Regional d'Aquitaine for financial support and the "Molecular Magnetic Materials" team in the CRPP for their help.

References

1 *Solid-state Supramolecular Chemistry: Two- and Three-Dimensional Inorganic Networks*, Comprehensive Supramolecular Chemistry, eds. J. L. Atwood, S. D. MacNicol, J. E. Davies, F. Vögtle, G. Alberti and T. Bein, Pergamon, Oxford, 1996, vol. 7.
2 (*a*) T. J. Barton, L. M. Bull, W. G. Klemperer, D. A. Loy, B. McEnaney, M. Misono, P. A. Monson, G. Pez, G. W. Scherer, J. C. Vartuli and O. M. Yaghi, *Chem. Mater.*, 1999, **11**, 2633; (*b*) M. E. Davis, *Nature*, 2002, **471**, 813; (*c*) G. J. de A. A. Soler-Illia, C. Sanchez, B. Lebeau and J. Patarin, *Chem. Rev.*, 2002, **102**, 4093.
3 (*a*) J. S. Beck and J. C. Vartuli, *Curr. Opin. Solid State Mater. Sci.*, 1996, **1**, 76; (*b*) N. K. Raman, M. T. Anderson and C. J. Brinker, *Chem. Mater.*, 1996, **8**, 1682; (*c*) A. Corma, *Chem. Rev.*, 1997, **97**, 2373; (*d*) J. Y. Ying, C. P. Mehnert and M. S. Wong, *Angew. Chem., Int. Ed. Engl.*, 1999, **28**, 56; (*e*) U. Ciesla and F. Schüth, *Micropor. Mesopor. Mater.*, 1999, **27**, 131.
4 (*a*) K. Moller and T. Bein, *Chem. Mater.*, 1998, **10**, 2950; (*b*) T. Asefa, C. Yoshina-Ishii, M. J. MacLachlan and G. A. Ozin, *J. Mater. Chem.*, 2000, **10**, 1751; (*c*) D. Trong On, D. Desplantier-Giscard, C. Danumah and S. Kaliaguine, *Appl. Catal. A*, 2001, **222**, 299; (*d*) A. P. Wright and M. E. Davis, *Chem. Rev.*, 2002, **102**, 3589.
5 (*a*) A. Corma, V. Fornés, H. Garcia, M. A. Miranda and M. J. Sabater, *J. Am. Chem. Soc.*, 1994, **116**, 9767; (*b*) F. Marlow, M. D. McGehee, D. Zhao, B. F. Chmelka and G. D. Stucky, *Adv. Mater.*, 1999, **11**, 632; (*c*) K. Moller, T. Bein and R. X. Fischer, *Chem. Mater.*, 1999, **11**, 665; (*d*) M. H. Lim and A. Stein, *Chem. Mater.*, 1999, **11**, 3285; (*e*) H. Hata, S. Saeki, T. Kimura, Y. Sugahara and K. Kuroda, *Chem. Mater.*, 1999, **11**, 1110; (*f*) M. Vallet-Regi, A. Ramila, R. P. del Real and J. Perez-Pariente, *Chem. Mater.*, 2001, **13**, 308; (*g*) J. Felipe Diaz and K. J. Balkus, Jr., *J. Mol. Catal. B: Enzymatic*, 1996, **2**, 115; (*h*) H. H. H. P. Yiu, P. A. Wright and N. P. Botting, *J. Mol. Catal. B: Enzymatic*, 2001, **15**, 81; (*i*) C.-H. Lee, T.-S. Lin, H.-P. Lin, Q. Zhao, S.-B. Liu and C.-Y. Mou, *Micropor. Mesopor. Mater.*, 2003, **57**, 199.
6 (*a*) H. B. Jervis, M. E. Raimondi, R. Raja, T. Maschmeyer, J. M. Seddon and D. W. Bruce, *J. Chem. Soc., Chem. Commun.*, 1999, 2031; (*b*) M. Ogawa, T. Nakamura, J.-I. Mori and K. Kuroda, *Micropor. Mesopor. Mater.*, 2001, **48**, 159; (*c*) Y. Tanamura, T. Uchida, N. Teramae, M. Kikuchi, K. Kusaba and Y. Onodera, *Nano Lett.*, 2001, **1**, 387; (*d*) K. Kageyama, J. Tamazawa and T. Aida, *Science*, **285**, 3113; (*e*) B. J. S. Johnson and A. Stein, *Inorg. Chem.*, 2001, **40**, 801; (*f*) W. Xu, Q. Luo, H. Wang, L. C. Francesconi, R. E. Stark and D. L. Akins, *J. Phys. Chem. B*, 2003, **107**, 497; (*g*) S. T. Bromley, G. Sankar, C. R. A. Catlow, J. M. Thomas and T. Maschmeyer, *Micropor. Mesopor. Mater.*, 2001, **44–45**, 395; (*h*) M. Hartmann, C. Bischof, Z. Luan and L. Kevan, *Micropor. Mesopor. Mater.*, 2001, **44–45**, 385; (*i*) R. J. P. Corriu, E. Lancelle-Beltean, A. Mehdi, C. Reyé, S. Brandas and R. Guilard, *J. Mater. Chem.*, 2002, **12**, 1355.
7 T. Coradin, J. Larionova, A. A. Smith, G. Rogez, R. Clérac, Ch. Guérin, G. Blondin, R. E. P. Winpenny, C. Sanchez and T. Mallah, *Adv. Mater.*, 2002, **14**, 896.
8 D. Gatteschi and R. Sessoli, *Angew. Chem., Int. Ed. Engl.*, 2003, **42**, 268.
9 R. Sessoli, D. Gatteschi, A. Caneschi and M. A. Novak, *Nature*, 1993, **365**, 141.
10 J. L. Friedman, M. P. Sarachik, J. Tejeda and R. Ziolo, *Phys. Rev. Lett.*, 1996, **76**, 3830.
11 W. Wernsdorfer and R. Sessoli, *Science*, 1999, **284**, 133.
12 H. J. Eppley, H.-L. Tsai, N. De Vries, K. Folting, G. Christou and D. N. Hendrickson, *J. Am. Chem. Soc.*, 1995, **117**, 301.
13 L. Krusin-Elbaum, T. Shibauchi, B. Argyle, L. Gignac and D. Weller, *Nature*, 2001, **410**, 444.
14 (*a*) E. M. Chudnovsky and J. Tejada, *Macroscopic Quantum Tunneling of the Magnetic Moment*, Cambrige University Press, Cambrige, 1998; (*b*) E. Fel Barco, N. Vernier, J. M. Hermnandy, J. Tejada, E. M. Chudrovsky and E. Molins, *Europhys. Lett.*, 1999, **47**, 722.
15 (*a*) M. Clemente-Leon, H. Soyer, E. Coronado, C. Mingotaud, C. J. Gomez-Garcia and P. Delhaès, *Angew. Chem., Int. Ed. Engl.*, 1998, **37**, 2842; (*b*) E. Coronado and C. Mingotaud, *Adv. Mater.*, 1999, **10**, 869.
16 D. Ruiz-Molina, M. Mas Torrent, J. Tejada, M. T. Martinez, C. Rovira and J. Veciana, *Adv. Mater.*, 2003, **15**, 42.
17 T. Lis, *Acta Cryst.*, 1980, **B36**, 2042.
18 (*a*) D. Gatteschi, A. Caneschi, L. Pardi and R. Sessoli, *Science*, 1994, **265**, 1054; (*b*) R. Sessoli, D. Gatteschi, A. Caneschi and M. A. Novak, *Nature*, 1993, **365**, 141.
19 J. Eppley, H.-L. Tsai, N. de Vries, K. Folting, G. Christou and D. N. Hendrickson, *J. Am. Chem. Soc.*, 1995, **117**, 301.

20 J. Yoo, E. K. Brechin, A. Yamaguchi, M. Nakano, J. C. Huffman, A. L. Maniero, L.-C. Brunel, K. Awaga, H. Ishimoto, G. Christou and D. N. Hendrickson, *Inorg. Chem.*, 2000, **39**, 3615.
21 D. Zhao, Q. Huo, J. Feng, B. F. Chmelka and G. D. Stucky, *J. Am. Chem. Soc.*, 1998, **120**, 6024.
22 S. Brunauer, P. H. Emmett and E. Teller, *J. Am. Chem. Soc.*, 1938, **60**, 309.
23 E. P. Barrett, L. G. Joyner and P. H. Halenda, *J. Am. Chem. Soc.*, 1951, **73**, 37.
24 E. A. Boudreaux and L. N. Mulay, *Theory and Applications of Molecular Paramagnetism*, John Wiley & Sons, New York, 1976.
25 K. S. W. Sing, D. H. Everett, R. A. W. Haul, L. Moscou, R. A. Pierotti, J. Rouquerol and T. Siemieniewska, *Pure Appl. Chem.*, 1985, **57**, 603.
26 J. Larionova, R. Clérac, B. Boury, J. Le Bideau, L. Lecren and S. Willemin, *J. Mater. Chem.*, 2003, **13**, 795.
27 (*a*) Z. Sun, D. Ruiz, N. R. Dilley, M. Soler, J. Ribas, K. Folting, M. B. Maple, G. Christou and D. N. Hendrickson, *Chem. Commun.*, 1999, 1973; (*b*) Z. Sun, H. J. Eppley, E. M. Rumberger, I. A. Guzei, K. Folting, P. K. Gantzel, A. L. Rheingold, G. Christou and D. N. Hendrickson, *Inorg. Chem.*, 2001, **40**, 2127.